The fact that the change in nuclear radii caused by addition of pairs of neutrons (the odd-even effect is attributable to other details of nuclear structure), is less than the empirical formulas predict—either the crude $A^{1/3}$ or the more elaborate expression—has been examined in terms of the possible effects of nuclear compressibility and changes in surface and volume-symmetry energies. Bodmer's[23] detailed examination of this matter suggests a much smaller compressibility energy than might be expected for general considerations. Additional evidence for such a "soft" nucleus is also provided by the analysis (Greiner and Scheck[24]) of muonic x-ray measurements of neighboring elements by Quitman *et al.*[25]

We conclude that the muonic isotope shifts confirm some of the conclusions of the optical measurements, and in principle enable this type of investigation to be extended to lighter nuclei. The development of improved γ-detection techniques now makes it possible to consider more extensive and more precise measurements.

Note added in proof. Recent measurements of the difference in the scattering of 250-MeV electrons by Ca^{40} and Ca^{44} indicate a difference in charge distribution for the two nuclei which is in good agreement with that reported in this paper. [R. Hofstadter *et al.*, Phys. Rev. Letters **15**, 758 (1965).]

[23] A. R. Bodmer, Nucl. Phys. **9**, 371 (1958).
[24] W. Greiner and F. Scheck, Nucl. Phys. **41**, 424 (1964).
[25] D. Quittmann, R. Engler, V. Hegel, P. Brix, G. Backenstoss, K. Goebel, and B. Stadler, Nucl. Phys. **51**, 609 (1964).

PHYSICAL REVIEW VOLUME 141, NUMBER 1 JANUARY 1966

Hyperfine Separation of Deuterium*

S. B. CRAMPTON,† H. G. ROBINSON,‡ D. KLEPPNER,§ AND N. F. RAMSEY
Harvard University, Cambridge, Massachusetts
(Received 15 July 1965)

The hyperfine separation of deuterium has been measured by a spin-exchange technique in which deuterium interacts with radiating hydrogen in a hydrogen maser. Resonance of the deuterium is detected by its effect on the hydrogen oscillation power level. The result is $\Delta\nu(\mathrm{D}) = 327\,384\,352.3 \pm 0.25$ cps in the $A1$ time scale [$\Delta\nu(\mathrm{Cs}) = 9\,192\,631\,770$ cps]. A theoretical analysis of the technique and experimental details are presented.

I. INTRODUCTION

THIS paper describes a redetermination of the ground-state hyperfine separation of deuterium by a new technique in which a hydrogen maser[1–3] is used as a polarization detector. The maser oscillates on the hydrogen hyperfine transition $(F=1, m_F=1) \rightarrow (F=0, m_F=0)$ at approximately 1420 Mc/sec. Spin-exchange collisions between deuterium and hydrogen relax the oscillating hydrogen magnetic moment by an amount depending on the deuterium electron polarization as well as on the spin-exchange collision rate. When a radiation field is applied at a deuterium resonance frequency, the deuterium electron polarization decreases and there is a corresponding decrease in the oscillating hydrogen magnetic moment. Changes in the maser power level thus serve to detect deuterium resonances.

This technique is similar to the optical-pumping spin-exchange method[4] in that changes in the deuterium electron polarization are detected by spin-exchange coupling to a second spin system whose electron polarization is more conveniently observed. However, it preserves two advantages of the hydrogen maser: The frequency shifts due to wall collisions are small relative to those produced by buffer-gas collisions in an optical-pumping experiment, and better spatial averaging of the magnetic-field gradients reduces the resonance linewidth and produces a highly symmetric line.

In principle, the deuterium hyperfine separation could have been measured with equal precision using a deuterium maser. However, there are substantial experimental difficulties associated with construction of such a maser owing mainly to the relatively low deuterium hyperfine frequency. The present method was chosen for its experimental simplicity, its interesting

* Work supported by the National Science Foundation and the Office of Naval Research.
† National Science Foundation Predoctoral Fellow during the period of this research. Present address: Department of Physics, Williams College, Williamstown, Mass.
‡ Yale University Faculty Fellow during the period of this research. Present address: Department of Physics, Duke University, Durham, North Carolina.
§ Alfred P. Sloan Foundation Fellow.
[1] D. Kleppner, H. M. Goldenberg, and N. F. Ramsey, Appl. Opt. **1**, 55 (1962).
[2] D. Kleppner, H. M. Goldenberg, and N. F. Ramsey, Phys. Rev. **126**, 601 (1962).
[3] D. Kleppner, H. C. Berg, S. B. Crampton, N. F. Ramsey, R. F. C. Vessot, H. E. Peters, and J. Vanier, Phys. Rev. **138**, A972 (1965).
[4] H. G. Dehmelt, Phys. Rev. **109**, 381 (1958); F. G. Major, thesis, University of Washington, 1962 (unpublished).

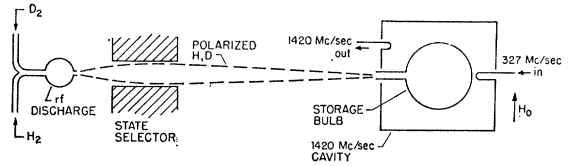

FIG. 1. Schematic diagram of the apparatus. Magnetic shields surrounding the cavity have been omitted for clarity.

relation to the optical-pumping spin-exchange method, and the ease with which it can be extended to the study of other paramagnetic atoms. In addition to the present measurement, this method has been used to determine the N^{14} quadrupole coupling constant,[5] and it should prove useful for certain other atomic systems.

The theory of the experiment has been derived in detail by Crampton[6] and will be summarized below. Preliminary results of this work have been reported previously.[7]

II. THE HYDROGEN MASER AS A SPIN-EXCHANGE SPECTROMETER

Since the hydrogen maser has been described in detail elsewhere,[1–3] the present description concentrates on features unique to this experiment.

A schematic diagram is shown in Fig. 1. Hydrogen and deuterium are mixed and dissociated in an rf discharge. The emerging atoms pass through a hexapole magnet which focuses into a beam those atoms possessing negative electron moments. By inspection of the energy levels of ground-state atomic hydrogen and deuterium, Fig. 2, it can be shown that the beam contains atoms in the following states (designated by F, m_F): hydrogen in states (1,1) and (1,0) and deuterium in states $(\frac{3}{2},\frac{3}{2})$, $(\frac{3}{2},\frac{1}{2})$, and $(\frac{3}{2},-\frac{1}{2})$. The atoms enter a 6-in.-diam spherical quartz storage bulb lined with TFE Teflon. They leave after a mean storage time of about $\frac{1}{3}$ sec, during which they cross the bulb about 10^4 times. The storage bulb is centered in a cylindrical cavity tuned to the hydrogen hyperfine frequency, and a static magnetic field (indicated by H_0 in Fig. 1) is applied transverse to the cavity axis in order to couple the cavity to the hydrogen transition $(F=1, m_F=1) \rightarrow (F=0, m_F=0)$. Transitions between deuterium hyperfine levels are induced by a second rf field at approximately 327 Mc/sec. This field is applied by a small loop (shown to the right of the storage bottle in Fig. 1) placed so as not to disturb the cavity mode seriously.

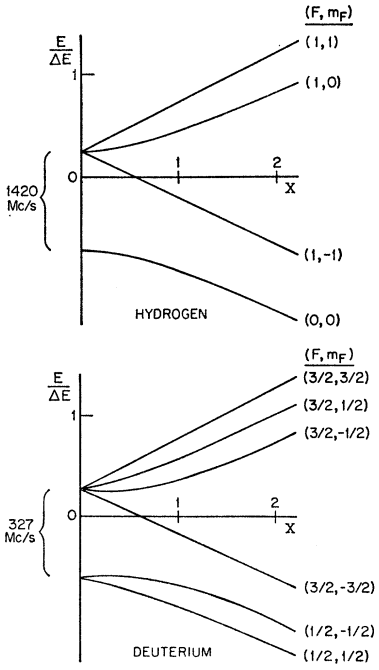

FIG. 2. Ground-state energy levels of H and D. $X=(-\mu_J/J+\mu_I/I)H_0/\Delta E$.

Sensitivity of the hydrogen oscillation level to deuterium resonances depends in a rather complicated manner on the various relaxation mechanisms which couple the hydrogen levels and limit the radiative lifetime. A detailed description of detection of the deuterium transition $(\frac{3}{2},\frac{3}{2}) \rightarrow (\frac{1}{2},\frac{1}{2})$ by its effect on the oscillation level of the hydrogen transition (1,1) → (0,0) is given in the next section, but by way of introduction a simplified discussion is presented here.

The radiation rate of hydrogen in the maser depends on the population difference of the levels concerned, as well as on the radiative lifetime and other factors such as hydrogen flux and cavity Q. With sufficient deuterium flux spin-exchange collisions decrease both the population difference and radiative lifetime, and there is a corresponding decrease in the power level.

The selection rule governing magnetic dipole transitions is $\Delta m_F=0, \pm 1$. Most previous hydrogen-maser experiments made use of the $\Delta m_F=0$ transition (1,0) → (0,0) because its frequency has no first-order dependence on the magnetic field. That transition is not suitable here, since it is insensitive to the deuterium populations and, hence, cannot be used to detect transitions between deuterium levels. This is a consequence of the fact that the hydrogen states (1,0) and (0,0) possess no z component of angular momentum, and there is consequently no preferred direction for a positive or negative polarization in the deuterium spin system. In contrast, the rate of radiation on the transition (1,1) → (0,0) does depend on the electron polarizations of the colliding atoms. (The electron polarization is twice the expectation value of z component of electron spin.) The (1,1) → (0,0) oscillation level can thereby serve to detect changes of electron polarization caused by a second rf field resonant at one of the deuterium hyperfine or Zeeman transition frequencies.

[5] H. G. Robinson, H. C. Berg, and S. B. Crampton, Bull. Am. Phys. Soc. 9, 564 (1964).
[6] S. B. Crampton, thesis, Harvard University, 1964 (unpublished).
[7] S. B. Crampton, D. Kleppner, and H. G. Robinson, Bull. Am. Phys. Soc. 8, 351 (1963).

The effect of a deuterium transition on the hydrogen oscillation level depends on the extent to which it changes the deuterium electron polarization. The problem is first to find the deuterium populations and then to calculate the effects of possible transitions on the electron polarization. This can be done readily in two limiting cases—the case when the densities of hydrogen and deuterium are sufficiently low that the rate of D-D and D-H spin-exchange collisions are small compared to the rate at which deuterium enters and leaves the storage bulb, and the opposite case of high densities when the collision rates are large.

Case I: Low Density

In this case, the deuterium level population differences are determined primarily by those of the incoming deuterium beam, though they are somewhat reduced by relaxation processes within the storage bulb. The preferentially occupied deuterium levels are $F=\frac{3}{2}$, $m_F=\frac{3}{2}$, $\frac{1}{2}$, $-\frac{1}{2}$. The hyperfine transitions which affect the electron polarization are $(\frac{3}{2},\frac{3}{2})\rightarrow(\frac{1}{2},\frac{1}{2})$, $(\frac{3}{2},\frac{1}{2})\rightarrow(\frac{1}{2},\frac{1}{2})$, and $(\frac{3}{2},-\frac{1}{2})\rightarrow(\frac{1}{2},-\frac{1}{2})$. (The field-independent transitions $(\frac{3}{2},\frac{1}{2})\rightarrow(\frac{1}{2},-\frac{1}{2})$ and $(\frac{3}{2},-\frac{1}{2})\rightarrow(\frac{1}{2},\frac{1}{2})$ do not change the electron polarization.) Of the three observable hyperfine transitions, the first, $(\frac{3}{2},\frac{3}{2})\rightarrow(\frac{1}{2},\frac{1}{2})$, affects the polarization twice as much as either of the others.

Case II: High Density

In the limit that spin exchange dominates all other transition mechanisms, the atoms become distributed among the spin levels so that the populations are proportional to $\exp\beta m_F$, where β depends on the z component of angular momentum of the entire atomic system.[8,9] In this limit, all deuterium transitions for which $\Delta m_F=-1$ produce the same change in electron polarization. The observable hyperfine transitions are $(\frac{3}{2},\frac{3}{2})\rightarrow(\frac{1}{2},\frac{1}{2})$, $(\frac{1}{2},-\frac{1}{2})\rightarrow(\frac{3}{2},-\frac{3}{2})$, and the two field-independent transitions $(\frac{3}{2},\frac{1}{2})\rightarrow(\frac{1}{2},-\frac{1}{2})$ and $(\frac{1}{2},\frac{1}{2})\rightarrow(\frac{3}{2},-\frac{1}{2})$. The last two transitions are unresolved at the low fields used and have a combined effect twice that of either field-dependent transition.

It might appear from these considerations that from the standpoint of signal intensity at moderate spin-exchange line widths, the most favorable deuterium hyperfine transition is the field-dependent transition $(\frac{3}{2},\frac{3}{2})\rightarrow(\frac{1}{2},\frac{1}{2})$. There are, however, two other considerations. The first is that, in addition to broadening the resonance, spin-exchange collisions can shift the resonance frequency. The second is that the field-dependent deuterium resonances must be corrected to zero magnetic field, which means that an accurate determination of the magnetic field is necessary. The unresolved field-independent transitions are substantially free from these complications, even at high exchange collision rates and are consequently most favorable. Observations were made in this experiment of both the field-dependent and field-independent transition. Details of the above considerations are given in the following section.

III. THEORY

A. Introduction

The system of interest is a gaseous combination of hydrogen and deuterium undergoing spin exchange with itself and interacting with applied radiation fields and various relaxation mechanisms. A complete description of the system can be given in terms of $\rho(\mathrm{H})$ and $\rho(\mathrm{D})$, the spin-state density matrices for hydrogen and deuterium, respectively.[10,11] Once $\rho(\mathrm{H})$ and $\rho(\mathrm{D})$ are known, it is a straightforward matter to derive expectation values for any desired experimental quantity such as the oscillating magnetization, polarization, etc.

The evolution in time of $\rho(\mathrm{H})$ is governed by rate equations which couple the two matrices. We formally identify the contributions to the time rate of change of $\rho(\mathrm{H})$ and $\rho(\mathrm{D})$, as follows:

$$\frac{d\rho(\mathrm{H})}{dt}=\left(\frac{d\rho(\mathrm{H})}{dt}\right)_{\text{flow}}+\left(\frac{d\rho(\mathrm{H})}{dt}\right)_{\text{radiation}}+\left(\frac{d\rho(\mathrm{H})}{dt}\right)_{\text{relaxation}}+\left(\frac{d\rho(\mathrm{H})}{dt}\right)_{\text{H-exchange}}+\left(\frac{d\rho(\mathrm{H})}{dt}\right)_{\text{D-exchange}}. \quad (1)$$

The first term represents the flow of hydrogen atoms in and out of the storage bulb. The second accounts for the interaction with the radiation field. The third describes the effect of all relaxation mechanisms, other than exchange, such as magnetic field inhomogeneties or wall imperfections. The fourth term accounts for hydrogen-hydrogen spin-exchange collisions, while the last accounts for hydrogen-deuterium exchange collisions. It is this last term which couples the hydrogen and deuterium systems.

The equation for the rate of change of the deuterium density matrix is similar:

$$\frac{d\rho(\mathrm{D})}{dt}=\left(\frac{d\rho(\mathrm{D})}{dt}\right)_{\text{flow}}+\left(\frac{d\rho(\mathrm{D})}{dt}\right)_{\text{radiation}}+\left(\frac{d\rho(\mathrm{D})}{dt}\right)_{\text{relaxation}}+\left(\frac{d\rho(\mathrm{D})}{dt}\right)_{\text{H-exchange}}+\left(\frac{d\rho(\mathrm{D})}{dt}\right)_{\text{D-exchange}}. \quad (2)$$

[8] L. W. Anderson, F. M. Pipkin, and J. C. Baird, Phys. Rev. **120**, 1279 (1960); **121**, 1864 (1961); **122**, 1962 (1961).
[9] L. W. Anderson, F. M. Pipkin, and J. C. Baird, Phys. Rev. **116**, 87 (1959).
[10] P. L. Bender, Phys. Rev. **132**, 2154 (1963).
[11] L. C. Balling, R. J. Hanson, and F. M. Pipkin, Phys. Rev. **133**, A607 (1964); **135**, AB1 (1964).

For clarity, $\rho(\mathrm{H})$ and $\rho(\mathrm{D})$ are displayed below, with the states explicitly identified by their value of F and m_F.

$$\rho(\mathrm{H})\equiv\begin{array}{c}(F,m_F)\\(1,1)\\(1,0)\\(1,-1)\\(0,0)\end{array}\begin{array}{c}\begin{array}{cccc}(1,1) & (1,0) & (1,-1) & (0,0)\end{array}\\\begin{bmatrix}H_{11} & H_{12} & H_{13} & H_{14}\\ H_{21} & H_{22} & H_{23} & H_{24}\\ H_{31} & H_{32} & H_{33} & H_{34}\\ H_{41} & H_{42} & H_{43} & H_{44}\end{bmatrix}\end{array}, \tag{3}$$

$$\rho(\mathrm{D})\equiv\begin{array}{c}(F,m_F)\\(\frac{3}{2},\frac{3}{2})\\(\frac{3}{2},\frac{1}{2})\\(\frac{3}{2},-\frac{1}{2})\\(\frac{3}{2},-\frac{3}{2})\\(\frac{1}{2},\frac{1}{2})\\(\frac{1}{2},-\frac{1}{2})\end{array}\begin{array}{c}\begin{array}{cccccc}(\frac{3}{2},\frac{3}{2}) & (\frac{3}{2},\frac{1}{2}) & (\frac{3}{2},-\frac{1}{2}) & (\frac{3}{2},-\frac{3}{2}) & (\frac{1}{2},\frac{1}{2}) & (\frac{1}{2},-\frac{1}{2})\end{array}\\\begin{bmatrix}D_{11} & D_{12} & D_{13} & D_{14} & D_{15} & D_{16}\\ D_{21} & D_{22} & D_{23} & D_{24} & D_{25} & D_{26}\\ D_{31} & D_{32} & D_{33} & D_{34} & D_{35} & D_{36}\\ D_{41} & D_{42} & D_{43} & D_{44} & D_{45} & D_{46}\\ D_{51} & D_{52} & D_{53} & D_{54} & D_{55} & D_{56}\\ D_{61} & D_{62} & D_{63} & D_{64} & D_{65} & D_{66}\end{bmatrix}\end{array}. \tag{4}$$

$\rho(\mathrm{H})$ and $\rho(\mathrm{D})$ represent mixed states due to the random histories of the atoms.

In the following sections, we will display explicitly those terms of Eqs. (1) and (2) which are needed to determine the effect of the deuterium resonance $(\frac{3}{2},\frac{3}{2})\rightarrow(\frac{1}{2},\frac{1}{2})$ on the power radiated by the hydrogen on the transition $(1,1)\rightarrow(0,0)$. Since these transitions are well resolved at the magnetic field used, off-diagonal elements corresponding to all other transitions will be omitted. The results of a similar analysis for the deuterium field-independent transitions, $(\frac{3}{2},\frac{1}{2})\rightarrow(\frac{1}{2},-\frac{1}{2})$ and $(\frac{1}{2},\frac{1}{2})\rightarrow(\frac{3}{2},-\frac{1}{2})$, is presented in the Appendix, along with an analysis of the experiment using the maser as an amplifier.

For convenience, we will display the exchange and nonexchange terms of $d\rho/dt$ separately.

B. Nonexchange Contributions to $d\rho/dt$

If we designate the mean lifetime of a hydrogen atom in the storage bulb by T_{HB}, we have[10]

$$\left(\frac{d\rho(\mathrm{H})}{dt}\right)_{\mathrm{flow}}=\frac{1}{T_{HB}}\begin{bmatrix}\frac{1}{2} & & & \\ & \frac{1}{2} & & \\ & & 0 & \\ & & & 0\end{bmatrix}-\frac{1}{T_{HB}}\rho(\mathrm{H}), \tag{5}$$

where all elements of ρ not shown are taken to be 0.

Significant contributions to $(d\rho/dt)_{\mathrm{rad}}$ arise when the applied oscillating field, $\mathbf{H}_1\cos\omega t$, is such that $\omega_{\mathrm{H}}\simeq\omega_{\mathrm{H0}}=(E_m-E_n)/\hbar$, where m and n refer to the states of interest. The matrix element (in units of frequency) connecting the states is taken to be of the form $\frac{1}{2}x_{\mathrm{H}}e^{i\omega_{\mathrm{H}}t}$. For the hydrogen transition $(1,1)\rightarrow(0,0)$,

$$x_{\mathrm{H}}=-\mu_0H_1/\sqrt{2}\hbar. \tag{6}$$

$\mathbf{H}_1$ is perpendicular to the static field $\mathbf{H}_0$. It is readily shown[10] that, neglecting the counter-rotating field,

$$(\dot{H}_{11})_{\mathrm{rad}}=-(\dot{H}_{44})_{\mathrm{rad}}=-x_{\mathrm{H}}\,\mathrm{Im}(H_{41}e^{-i\omega_{\mathrm{H}}t}) \tag{7a}$$

$$(\dot{H}_{41})_{\mathrm{rad}}=(\dot{H}_{14}{}^*)_{\mathrm{rad}}=i\omega_0H_{41}+(i/2)x_{\mathrm{H}}(H_{11}-H_{44})e^{i\omega_{\mathrm{H}}t}. \tag{7b}$$

We describe relaxation processes other than spin exchange by times T_1 and T_2, which account for relaxation of the diagonal and off-diagonal elements, respectively. The form of the relaxation is taken to be simple decay to the equilibrium value. (This is an oversimplification. For instance, Zeeman relaxation does not couple states with different F. However, we believe that these approximations introduce no serious errors; they can be removed, but only at the cost of considerable algebra.) Thus, for hydrogen we have the relaxation terms

$$\dot{H}_{mm}=T_{\mathrm{H1}}{}^{-1}[\tfrac{1}{4}-H_{mm}], \tag{8a}$$

$$\dot{H}_{41}=-T_{\mathrm{H2}}{}^{-1}H_{41}. \tag{8b}$$

Combining Eqs. (5), (7), and (8), we obtain for the nonexchange contributions to $\dot{\rho}(H)$:

$$\dot{H}_{11}=T_{HB}{}^{-1}[\tfrac{1}{2}-H_{11}]+T_{\mathrm{H1}}{}^{-1}[\tfrac{1}{4}-H_{11}]-x_{\mathrm{H}}\,\mathrm{Im}(H_{41}e^{-i\omega_{\mathrm{H}}t}), \tag{9a}$$

$$\dot{H}_{22}=T_{HB}{}^{-1}[\tfrac{1}{2}-H_{22}]+T_{\mathrm{H1}}{}^{-1}[\tfrac{1}{4}-H_{22}], \tag{9b}$$

$$\dot{H}_{33}=-T_{HB}{}^{-1}H_{33}+T_{\mathrm{H1}}{}^{-1}[\tfrac{1}{4}-H_{33}], \tag{9c}$$

$$\dot{H}_{44}=-T_{HB}{}^{-1}H_{44}+T_{\mathrm{H1}}{}^{-1}[\tfrac{1}{4}-H_{44}]+x_{\mathrm{H}}\,\mathrm{Im}(H_{41}e^{-i\omega_{\mathrm{H}}t}), \tag{9d}$$

$$\dot{H}_{41}=-(T_{HB}{}^{-1}+T_{\mathrm{H2}}{}^{-1}-i\omega_{\mathrm{H0}})H_{41}+(i/2)x_{\mathrm{H}}(H_{11}-H_{44})e^{i\omega_{\mathrm{H}}t}. \tag{9e}$$

The nonexchange contribution to $d\rho(\mathrm{D})/dt$ is similar. Let ω_{D0} be the frequency of the transition $(\frac{3}{2},\frac{3}{2})\rightarrow(\frac{1}{2},\frac{1}{2})$ and the matrix element driving it be $\frac{1}{2}x_{\mathrm{D}}e^{i\omega_{\mathrm{D}}t}$, where

$$x_{\mathrm{D}}=-(\sqrt{\tfrac{2}{3}})\mu_0H_1/\hbar. \tag{10}$$

H_1 here represents the amplitude of the rf field stimulating the deuterium transition. The results for

$(d\rho(\mathrm{D})/dt)_{\text{nonexchange}}$ are:

$$\dot{D}_{11}=T_{DB}^{-1}(\tfrac{1}{3}-D_{11})-x_{\mathrm{D}}\,\mathrm{Im}(D_{51}e^{-i\omega_{\mathrm{D}}t}) +T_{\mathrm{D1}}^{-1}(\tfrac{1}{6}-D_{11}), \quad (11a)$$

$$\dot{D}_{22}=T_{DB}^{-1}(\tfrac{1}{3}-D_{22})+T_{\mathrm{D1}}^{-1}(\tfrac{1}{6}-D_{22}), \quad (11b)$$

$$\dot{D}_{33}=T_{DB}^{-1}(\tfrac{1}{3}-D_{33})+T_{\mathrm{D1}}^{-1}(\tfrac{1}{6}-D_{33}), \quad (11c)$$

$$\dot{D}_{44}=-T_{DB}^{-1}D_{44}+T_{\mathrm{D1}}^{-1}(\tfrac{1}{6}-D_{44}), \quad (11d)$$

$$\dot{D}_{55}=-T_{DB}^{-1}D_{55}+x_{\mathrm{D}}\,\mathrm{Im}(D_{51}e^{-i\omega_{\mathrm{D}}t}) +T_{\mathrm{D1}}^{-1}(\tfrac{1}{6}-D_{55}), \quad (11e)$$

$$\dot{D}_{66}=-T_{DB}^{-1}D_{66}+T_{\mathrm{D1}}^{-1}(\tfrac{1}{6}-D_{66}), \quad (11f)$$

$$\dot{D}_{51}=-(T_{DB}^{-1}-i\omega_{\mathrm{D0}}+T_{\mathrm{D2}}^{-1})D_{51} +(i/2)x_{\mathrm{D}}(D_{11}-D_{55})e^{i\omega_{\mathrm{D}}t}. \quad (11g)$$

To illustrate the procedure for handling the full set of rate equations we will calculate the power radiated in the absence of exchange. In this case, $d\rho(\mathrm{H})/dt$ is completely given by Eqs. (9a)–(9e). We can solve these equations by combining them in the following form:

$$\dot{H}_{11}-\dot{H}_{44}=\tfrac{1}{2}T_{HB}^{-1}-(T_{HB}^{-1}+T_{\mathrm{H1}}^{-1})(H_{11}-H_{44}) -2x_{\mathrm{H}}\,\mathrm{Im}(H_{41}e^{-i\omega_{\mathrm{H}}t}), \quad (9f)$$

$$\dot{H}_{41}=-(T_{HB}^{-1}+T_{\mathrm{H2}}^{-1})H_{41}+i\omega_{0\mathrm{H}}H_{41} +(i/2)x_{\mathrm{H}}(H_{11}-H_{44})e^{i\omega_{\mathrm{H}}t}. \quad (9e)$$

For stationary oscillation, $\dot{H}_{11}-\dot{H}_{44}=0$, and the above equations are solved by the substitution

$$H_{41}=(\alpha+i\beta)e^{i\omega_{\mathrm{H}}t}, \quad (12)$$

where α and β are real numbers. The result is

$$\alpha=\frac{\tau_{\mathrm{H2}}'}{4T_{HB}} \times\frac{x_{\mathrm{H}}(\omega_{\mathrm{H}}-\omega_{\mathrm{H0}})}{(\tau_{\mathrm{H1}}'\tau_{\mathrm{H2}}')^{-1}+(\tau_{\mathrm{H2}}'/\tau_{\mathrm{H1}}')(\omega_{\mathrm{H}}-\omega_{0\mathrm{H}})^2+x_{\mathrm{H}}^2}. \quad (13)$$

$$\beta=\frac{1}{4T_{HB}} \times\frac{x_{\mathrm{H}}}{(\tau_{\mathrm{H1}}'\tau_{\mathrm{H2}}')^{-1}+(\tau_{\mathrm{H2}}'/\tau_{\mathrm{H1}}')(\omega_{\mathrm{H}}-\omega_{0\mathrm{H}})^2+x_{\mathrm{H}}^2}, \quad (14)$$

where

$$\frac{1}{\tau_{\mathrm{H1}}'}=\frac{1}{T_{\mathrm{H1}}}+\frac{1}{T_{HB}}, \quad (15)$$

$$\frac{1}{\tau_{\mathrm{H2}}'}=\frac{1}{T_{\mathrm{H2}}}+\frac{1}{T_{HB}}. \quad (16)$$

The power radiated by the ensemble is computed from the oscillating magnetization $\mathbf{M}$.

$$\mathbf{M}=n(\mathrm{H})\langle\boldsymbol{\mu}_{0p}\rangle=-g_j\mu_0 n(\mathrm{H})\langle\mathbf{J}\rangle =-g_j\mu_0 n(\mathrm{H})\,\mathrm{Tr}[\mathbf{J}\rho(\mathrm{H})], \quad (17)$$

where $n(\mathrm{H})$ is the hydrogen density.

The radiated power is given by

$$P=-\int\mathbf{M}\cdot\frac{d\mathbf{H}}{dt}d^3r=-V_B\left\langle M_X\frac{d}{dt}H_1\cos\omega_{\mathrm{H}}t\right\rangle_{\mathrm{av}} =n(\mathrm{H})V_B(\mu_0/\sqrt{2})H_1\omega\beta. \quad (18)$$

V_B is the volume of the radiating gas and

$$n(\mathrm{H})V_B=I_{\mathrm{H}}T_B, \quad (19)$$

where I_{H} is the total hydrogen flux. By combining Eqs. (6) and (14)–(19), we obtain the following:

$$P=\tfrac{1}{4}I_{\mathrm{H}}\hbar\omega \times\frac{x_{\mathrm{H}}^2}{(\tau_{\mathrm{H1}}'\tau_{\mathrm{H2}}')^{-1}+(\tau_{\mathrm{H2}}'/\tau_{\mathrm{H1}}')(\omega_{\mathrm{H}}-\omega_{\mathrm{H0}})^2+x_{\mathrm{H}}^2}. \quad (20)$$

C. Spin-Exchange Contributions to $d\varrho/dt$

A number of authors have undertaken investigations of spin exchange.[6,10–14] (A list of references is given in Ref. 11.) The analysis by Balling, Hanson, and Pipkin[11] (hereinafter referred to as BHP) can be readily applied to the present experiments. Their theory is in agreement with experiments on electron-rubidium collisions, though there appears to be a slight discrepancy in the case of electron-cesium collisions,[15] possibly due to the neglect of spin-orbit interaction. This effect is expected to be much smaller for atom-atom collisions. In any case, spin-exchange theory which ignores this effect has given good agreement in the case of hydrogen, both in experiments on spin exchange relaxation[16] and frequency shifts.[6,17] The conditions of these experiments were sufficiently close to the present for us to apply the theory with confidence.

The spin-exchange process is described in BHP by the spin-flip cross section σ_{SF} [BHP Eq. (25-1)] and the shift parameter κ [BHP Eq. (26)] defined by

$$\sigma_{\mathrm{SF}}=(\pi/\kappa^2)\sum_{l=0}^{\infty}(2l+1)\sin^2(\delta_l^3-\delta_l^1), \quad (21)$$

$$\kappa=\frac{1}{\sigma_{\mathrm{SF}}}\frac{\pi}{2k^2}\sum_{l=0}^{\infty}(2l+1)\sin[2(\delta_l^3-\delta_l^1)], \quad (22)$$

where δ_l^1 and δ_l^3 are the singlet and triplet phase shifts for binary collisions at angular momentum $\hbar l$ and relative momentum $\hbar\mathbf{k}$. For our purposes it is more convenient to introduce spin-exchange collision and

[12] E. M. Purcell and G. B. Field, Astrophys. J. **124**, 542 (1956).
[13] J. P. Wittke and R. H. Dicke, Phys. Rev. **103**, 620 (1956).
[14] J. P. Wittke, thesis, Princeton University, 1955 (unpublished).
[15] L. C. Balling and F. M. Pipkin, Phys. Rev. **136**, A46 (1964).
[16] H. C. Berg, Phys. Rev. **137**, A1621 (1965).
[17] S. B. Crampton and D. Kleppner, Bull. Am. Phys. Soc. **9**, 451 (1964). The last sentence of this reference should read: "Spin-exchange shifts of the order of 1% of a 40-cps change in linewidth of the $\Delta m_F=-1$ oscillation frequency and 0.5% of a 1-cps change in linewidth of the $\Delta m_F=0$ oscillation frequency are in agreement with a theoretical estimate of the spin-exchange-shift parameter . . . ."

frequency shift rates, T_{HD}^{-1} and $\kappa_{HD}T_{HD}^{-1}$, respectively, which are defined in the case of hydrogen colliding with deuterium by

$$T_{HD}^{-1}=n(D)\langle v_{rel}\sigma_{SF}(H,D)\rangle$$
$$=n(D)\left\langle\frac{\pi\hbar}{\mu k}\sum_{l=0}^{\infty}(2l+1)\sin^2(\delta_l^3-\delta_l^1)\right\rangle_k, \quad (23)$$

$$\kappa_{HD}T_{HD}^{-1}=n(D)\langle v_{rel}\kappa(H,D)\rangle$$
$$=n(D)\left\langle\frac{\pi\hbar}{2\mu k}\sum_{l=0}^{\infty}(2l+1)\sin[2(\delta_l^3-\delta_l^1)]\right\rangle_k. \quad (24)$$

μ is the reduced mass and $n(D)$ is the deuterium density. The average is over the thermal velocity distribution. Rates for the other collision combinations are similarly described and are denoted by T_{HH}^{-1}, T_{DH}^{-1}, etc. It is readily verified that

$$T_{DH}^{-1}=\frac{n(H)}{n(D)}T_{HD}^{-1},$$
$$\kappa_{DH}T_{DH}^{-1}=\frac{n(H)}{n(D)}\kappa_{HD}T_{HD}^{-1}. \quad (25)$$

We also introduce the symbols $\mathcal{P}(H)$ and $\mathcal{P}(D)$ for the electron polarization of the hydrogen and deuterium. If the electron has spin angular momentum $\mathbf{S}\hbar$, then $\mathcal{P}$ is defined by

$$\mathcal{P}=\langle S_z\rangle/S=2\langle M_z\rangle, \quad (26)$$

from which it follows that

$$\mathcal{P}(H)=2\,\mathrm{Tr}[S_z\rho(H)]=H_{11}-H_{33}, \quad (27)$$

$$\mathcal{P}(D)=2\,\mathrm{Tr}[S_z\rho(D)]=D_{11}+\tfrac{1}{3}D_{22}-\tfrac{1}{3}D_{33}-D_{44}-\tfrac{1}{3}D_{55}+\tfrac{1}{3}D_{66}. \quad (28)$$

A related quantity which will also be useful is the atomic polarization, $\mathcal{A}$. If the total atomic angular momentum is $F\hbar$, then

$$\mathcal{A}=\langle F_z\rangle=\langle M_F\rangle. \quad (29)$$

$\mathcal{A}$ is readily evaluated, with the following results:

$$\mathcal{A}(H)=\mathrm{Tr}m_{F2}(H)=H_{11}-H_{33}=\mathcal{P}(H), \quad (30)$$

$$\mathcal{A}(D)=\mathrm{Tr}F_z\rho(D)=\tfrac{3}{2}D_{11}+\tfrac{1}{2}D_{22}-\tfrac{1}{2}D_{33}-\tfrac{3}{2}D_{44}+\tfrac{1}{2}D_{55}-\tfrac{1}{2}D_{66}=\tfrac{3}{2}\mathcal{P}(D)+D_{55}-D_{66}. \quad (31)$$

To simplify notation, we temporarily drop the subscript "exchange" from $d\rho/dt$ and instead use subscripts to indicate the spin-exchange process being considered. Thus $\dot\rho(H)_{exchange}=\dot\rho(H)_{HH}+\dot\rho(H)_{HD}$, where $\dot\rho(H)_{HD}$ is the rate of change of the hydrogen density matrix due to spin-exchange collisions with deuterium. Our starting point is BHP Eq. (27). In evaluating $d\rho/dt$, we retain only those terms which make a significant contribution to subsequent calculations. In particular, terms contributed by nuclear identity [denoted by σ_{SF}' and $\sigma_{SF}'\kappa'$ in BHP Eq. (B2)] are omitted on the ground that they are very small compared to the terms retained. Terms involving squares of off-diagonal elements are dropped for the same reason.

A matrix for $\dot\rho(H)_{HH}$ is given in BHP, Table 10. With the assumptions stated above, their result can be reduced to $(d\dot\rho(H)/dt)_{HH}$:

$$\dot H_{11}=-T_{HH}^{-1}\{H_{11}-[1+\mathcal{P}(H)]^2/4\}, \quad (32a)$$

$$\dot H_{22}=-T_{HH}^{-1}\{H_{22}-[1-\mathcal{P}(H)^2]/4\}, \quad (32b)$$

$$\dot H_{33}=-T_{HH}^{-1}\{H_{33}-[1-\mathcal{P}(H)]^2/4\}, \quad (32c)$$

$$\dot H_{44}=-T_{HH}^{-1}\{H_{44}-[1-\mathcal{P}(H)^2]/4\}, \quad (32d)$$

$$\dot H_{41}=-T_{HH}^{-1}\{[(1-\mathcal{P}(H)]/2-(i/2)\kappa_{HH}[H_{11}-H_{44}-\mathcal{P}(H)]\}H_{41}. \quad (32e)$$

Equations for the remaining contributions to the spin-exchange terms in ρ can be found by a straightforward application of BHP Eq. (27). The results follow:

$(d\rho(H)/dt)_{HD}$:

$$\dot H_{11}=-T_{HD}^{-1}\{H_{11}-[1+\mathcal{P}(D)][1+\mathcal{P}(H)]/4\}, \quad (33a)$$

$$\dot H_{22}=-T_{HD}^{-1}\{H_{22}-[1-\mathcal{P}(D)\mathcal{P}(H)]/4\}, \quad (33b)$$

$$\dot H_{33}=-T_{HD}^{-1}\{H_{33}-[1-\mathcal{P}(D)][1-\mathcal{P}(H)]/4\}, \quad (33c)$$

$$\dot H_{44}=-T_{HD}^{-1}\{H_{44}-[1-\mathcal{P}(D)\mathcal{P}(H)]/4\}, \quad (33d)$$

$$\dot H_{41}=-T_{HD}^{-1}\{(3-\mathcal{P}(D))/4+(i/2)\kappa_{HD}\mathcal{P}(D)\}H_{41}. \quad (33e)$$

$(d\rho(D)/dt)_{DH}$:

$$\dot D_{11}=-T_{DH}^{-1}\{\tfrac{1}{2}[1-\mathcal{P}(H)]D_{11}-\tfrac{1}{6}[1+\mathcal{P}(H)][D_{22}+2D_{55}]\}, \quad (34a)$$

$$\dot D_{22}=-T_{DH}^{-1}\{\tfrac{1}{6}[1-\mathcal{P}(H)][-D_{11}+D_{22}]+\tfrac{1}{9}[1+\mathcal{P}(H)][-2D_{33}-D_{66}]+(5D_{22}-2D_{55})/9\}, \quad (34b)$$

$$\dot D_{33}=-T_{DH}^{-1}\{-\tfrac{1}{9}[1-\mathcal{P}(H)][2D_{22}+D_{55}]+\tfrac{1}{6}[1+\mathcal{P}(H)][D_{33}-D_{44}]+[5D_{33}-2D_{66}]/9\}, \quad (34c)$$

$$\dot D_{44}=-T_{DH}^{-1}\{-\tfrac{1}{6}[1-\mathcal{P}(H)][D_{33}+2D_{66}]+\tfrac{1}{2}[1+\mathcal{P}(H)]D_{44}\}, \quad (34d)$$

$$\dot D_{55}=-T_{DH}^{-1}\{-\tfrac{1}{3}[1-\mathcal{P}(H)]D_{11}-(1/18)[1+\mathcal{P}(H)][2D_{33}-3D_{55}+D_{66}]-[2D_{22}-5D_{55}]/9\}, \quad (34e)$$

$$\dot D_{66}=-T_{DH}^{-1}\{-(1/18)[1-\mathcal{P}(H)]\times[2D_{22}+D_{55}-3D_{66}]-\tfrac{1}{3}[1+\mathcal{P}(H)]D_{44}-[2D_{33}-5D_{66}]/9\}, \quad (34f)$$

$$\dot D_{51}=-\tfrac{1}{6}T_{DH}^{-1}\{5-\mathcal{P}(H)+4i\kappa_{DH}\mathcal{P}(H)\}D_{51}. \quad (34g)$$

$(d\rho(\mathrm{D})/dt)_{\mathrm{DD}}$:

$$\dot{D}_{11}=-T_{\mathrm{DD}}^{-1}\{\tfrac{1}{2}[1-\mathcal{P}(\mathrm{D})]D_{11}-\tfrac{1}{6}[1+\mathcal{P}(\mathrm{D})][D_{22}+2D_{55}]\}, \quad (35a)$$

$$\dot{D}_{22}=-T_{\mathrm{DD}}^{-1}\{-\tfrac{1}{6}[1-\mathcal{P}(\mathrm{D})][D_{11}-D_{22}]-\tfrac{1}{9}[1+\mathcal{P}(\mathrm{D})][2D_{33}+D_{66}]+(5D_{22}-2D_{55})/9\}, \quad (35b)$$

$$\dot{D}_{33}=-T_{\mathrm{DD}}^{-1}\{-\tfrac{1}{9}[1-\mathcal{P}(\mathrm{D})][2D_{22}+D_{55}]+\tfrac{1}{6}[1+\mathcal{P}(\mathrm{D})][D_{33}-D_{44}]+[5D_{33}-2D_{66}]/9\}, \quad (35c)$$

$$\dot{D}_{44}=-T_{\mathrm{DD}}^{-1}\{-\tfrac{1}{6}[1-\mathcal{P}(\mathrm{D})][D_{33}+2D_{66}]+\tfrac{1}{2}[1+\mathcal{P}(\mathrm{D})]D_{44}\}, \quad (35d)$$

$$\dot{D}_{55}=-T_{\mathrm{DD}}^{-1}\{-\tfrac{1}{3}[1-\mathcal{P}(\mathrm{D})]D_{11}-(1/18)[1+\mathcal{P}(\mathrm{D})][2D_{33}-3D_{55}+D_{66}]-\tfrac{1}{9}[2D_{22}-5D_{55}]\}. \quad (35e)$$

$$\dot{D}_{66}=-T_{\mathrm{DD}}^{-1}\{-(1/18)[1-\mathcal{P}(\mathrm{D})]\times[2D_{22}+D_{55}-3D_{66}]-\tfrac{1}{3}[1+\mathcal{P}(\mathrm{H})]\times[D_{44}-\tfrac{1}{9}(2D_{33}+5D_{66}]\}, \quad (35f)$$

$$\dot{D}_{51}=-\tfrac{1}{9}T_{\mathrm{DD}}^{-1}\{5D_{22}+8D_{33}+9D_{44}+4D_{55}+7D_{66}\}D_{51}+(2i/3)\kappa_{\mathrm{DD}}T_{\mathrm{DD}}^{-1}\times[D_{11}-D_{55}-\mathcal{P}(\mathrm{D})]D_{51}. \quad (35g)$$

The nature of the spin-exchange process can be readily understood if we temporarily neglect all nonexchange processes. The results are most succinctly and usefully stated in terms of the rate of change of the polarization. Combining Eqs. (32) and (33) yields

$$d\mathcal{P}(\mathrm{H})/dt=-T_{\mathrm{HD}}^{-1}[\mathcal{P}(\mathrm{H})-\mathcal{P}(\mathrm{D})]/2, \quad (36)$$

and, in a similar manner, Eqs. (34) and (35) yield

$$d\mathcal{A}(\mathrm{D})/dt=+T_{\mathrm{DH}}^{-1}[\mathcal{P}(\mathrm{H})-\mathcal{P}(\mathrm{D})]/2. \quad (37)$$

By incorporating Eq. (25) with the above, we obtain the following result for the rate of change of the z component of the total atomic angular momentum:

$$n(\mathrm{H})\frac{d\mathcal{A}(\mathrm{H})}{dt}+n(\mathrm{D})\frac{d\mathcal{A}(\mathrm{D})}{dt}=0. \quad (38)$$

It is apparent that the spin-exchange process drives the electron polarization of the two spin systems towards equilibrium, while at the same time it conserves the z component of the angular momentum of the whole system.

The steady-state solutions of Eqs. (36) and (37) lead to

$$\mathcal{P}(\mathrm{H})=\mathcal{P}(\mathrm{D})\equiv\mathcal{P}, \quad (39)$$

where $\mathcal{P}$ is the equilibrium polarization of the system. The stationary solutions to Eqs. (32)–(35) are then

$$H_{jj}=\tfrac{1}{4}(1-\mathcal{P}^2)\left[\frac{1+\mathcal{P}}{1-\mathcal{P}}\right]^{m_F(j)}, \quad (40)$$

$$D_{jj}=\frac{(1-\mathcal{P}^2)^{3/2}}{2(3+\mathcal{P}^2)}\left[\frac{1+\mathcal{P}}{1-\mathcal{P}}\right]^{m_F(j)}. \quad (41)$$

The subscript j stands for any hyperfine level and $m_F(j)$ is the value of m_F for that level. This illustrates the result of Anderson, Pipkin, and Baird[9] that the most probable distribution of level populations in an isolated system undergoing spin exchange is given by a Boltzmann distribution, $e^{\beta m_F}$.

The "spin temperature" β^{-1} is given in our case by[18]

$$\beta^{-1}=\ln[(1+\mathcal{P})/(1-\mathcal{P})]. \quad (42)$$

By substituting these results in the defining equations for $\mathcal{A}(\mathrm{H})$ and $\mathcal{A}(\mathrm{D})$, we obtain

$$\mathcal{A}(\mathrm{H})=\mathcal{P}, \quad (43)$$

$$\mathcal{A}(\mathrm{D})=\tfrac{1}{2}\mathcal{P}(11+\mathcal{P}^2)/(3+\mathcal{P}^2). \quad (44)$$

D. Oscillation Conditions for the Hydrogen Maser

In this section, we investigate oscillation of the maser on the hydrogen transition (1,1) → (0,0). Our procedure will be to equate the radiated power P to the power required to maintain the oscillating field. For the present, we will treat $\mathcal{P}(\mathrm{H})$ and $\mathcal{P}(\mathrm{D})$ as independent quantities.

We begin by solving the rate equations as in Sec. B.

$$\frac{d}{dt}(H_{11}-H_{44})=\tfrac{1}{2}\{T_{HB}^{-1}+T_{\mathrm{HH}}^{-1}\mathcal{P}(\mathrm{H})(1+\mathcal{P}(\mathrm{H}))+\tfrac{1}{2}T_{\mathrm{HD}}^{-1}[\mathcal{P}(\mathrm{D})+\mathcal{P}(\mathrm{H})+2\mathcal{P}(\mathrm{D})\mathcal{P}(\mathrm{H})]\}-[T_{HB}^{-1}+T_{H1}^{-1}+T_{\mathrm{HH}}^{-1}+T_{\mathrm{HD}}^{-1}](H_{11}-H_{44})-2x_{\mathrm{H}}\,\mathrm{Im}H_{41}e^{i\omega_{\mathrm{H}}t}, \quad (45)$$

$$\frac{d}{dt}H_{41}=-\{T_{HB}^{-1}+T_{H2}^{-1}+\tfrac{1}{2}T_{\mathrm{HH}}^{-1}[1-\mathcal{P}(\mathrm{H})]+\tfrac{1}{4}T_{\mathrm{HD}}^{-1}[3-\mathcal{P}(\mathrm{D})]\}H_{41}+i\{\omega_{\mathrm{H0}}+\tfrac{1}{2}\kappa_{\mathrm{HH}}T_{\mathrm{HH}}^{-1}(H_{11}-H_{44}-\mathcal{P}(\mathrm{H}))-\tfrac{1}{2}\kappa_{\mathrm{HD}}T_{\mathrm{HD}}^{-1}\mathcal{P}(\mathrm{D})\}H_{41}-\frac{i}{2}x_{\mathrm{H}}(H_{11}-H_{44})e^{i\omega_{\mathrm{H}}t}. \quad (46)$$

[18] We also find this form for β^{-1} to hold for the level populations of hydrogen in spin-exchange equilibrium with atoms having nuclear spin 1 and electron spin $\frac{3}{2}$ [N^{14}] and atoms having nuclear spin $\frac{1}{2}$ and electron spin 1, although in these latter cases $\mathcal{P}$ is not simply proportional to the expectation value of the electron spin of the nonhydrogen species.

These equations have the same form as Eqs. (9e), (9f), and the solution is

$$H_{41}e^{i\omega_H t}=\frac{Ax_H/2}{(\tau_{H1}\tau_{H2})^{-1}+(\tau_{H2}/\tau_{H1})(\omega_H-\omega_{H0}')^2+x_H^2}, \quad (47)$$

where

$$A=\tfrac{1}{2}\{T_{HB}^{-1}+T_{HH}^{-1}\mathcal{P}(H)[1+\mathcal{P}(H)] +\tfrac{1}{2}T_{HD}^{-1}[\mathcal{P}(D)+\mathcal{P}(H)+2\mathcal{P}(D)\mathcal{P}(H)]\}.$$

The resonant frequency ω_{H0}' is slightly shifted from ω_{H0} by spin exchange.[7] Thus the solution for radiated power corresponding to Eq. (20) is

$$P=\tfrac{1}{2}I_H T_{HB}\hbar\omega A \times\frac{x_H^2}{(\tau_{H1}\tau_{H2})^{-1}+(\tau_{H2}/\tau_{H1})(\omega_H-\omega_{H0}')^2+x_H^2}. \quad (48)$$

The energy density, and hence the radiated power, is proportional to x_H^2, and to simplify the equations we retain x_H as our dependent variable. For analyzing this experiment it is convenient to give the results in terms of the polarizations (as yet undetermined) and the relaxation times.

If we equate P to the power dissipated, and do some rearranging, we obtain

$$x_H^2=(mT_{HH})^{-1}\{T_{HB}^{-1}+T_{HH}^{-1}\mathcal{P}(H)(1+\mathcal{P}(H)) +\tfrac{1}{2}T_{HD}^{-1}[\mathcal{P}(D)+\mathcal{P}(H)+2\mathcal{P}(H)\mathcal{P}(D)]\} -\{T_{HB}^{-1}+T_{H1}^{-1}+T_{HH}^{-1}+T_{HD}^{-1}\} \times\{T_{HB}^{-1}+T_{H2}^{-1}+\tfrac{1}{2}T_{HH}^{-1}[1-\mathcal{P}(H)] +\tfrac{1}{4}T_{HD}^{-1}[3-\mathcal{P}(H)]\}. \quad (49)$$

The constant m is given by[19]

$$m=\frac{\sigma_{SF}(H,H)\bar{v}\hbar}{\pi\mu_0^2}\frac{V_c}{\eta V_b}\frac{1}{Q}, \quad (50)$$

where V_c=cavity volume, and $\eta=\langle H_1\rangle^2_{\text{bulb}}/\langle H^2\rangle_{\text{cavity}}$ (as explained in Ref. 2, Sec. IV.E). The beam flux appears implicitly in these equations through the collision rates T_{HH}^{-1} and T_{HD}^{-1}. These depend, respectively, on $n(H)$ and $n(D)$, which in turn depend on the hydrogen and deuterium flux.

E. Detection of the Deuterium Resonance

Our remaining task is to find $\mathcal{P}(H)$ and $\mathcal{P}(D)$ in the presence of the applied oscillatory fields. The procedure for hydrogen is straightforward; from Eqs. (9), (27), (32), and (33), we obtain

$$\frac{d\mathcal{P}(H)}{dt}=\tfrac{1}{2}T_{HB}^{-1}-(T_{HB}^{-1}+T_{H1}^{-1}+T_{HD}^{-1})\mathcal{P}(H) -\tfrac{1}{2}T_{HD}^{-1}[\mathcal{P}(H)-\mathcal{P}(D)]-x_H\,\mathrm{Im}H_{41}e^{-i\omega_x t}. \quad (51)$$

For stationary oscillation, $d\mathcal{P}(H)/dt=0$. By combining Eqs. (47), (49), and (51) and rearranging, we finally have

$$\mathcal{P}(H)=(a/b)+(1/2b)T_{HD}^{-1}\mathcal{P}(D), \quad (52)$$

where

$$a=\tfrac{1}{2}T_{HB}^{-1}-(\tfrac{1}{4}m)T_{HH}x_H^2, \qquad b=T_{HB}^{-1}+T_{H1}^{-1}+\tfrac{1}{2}T_{HD}^{-1}. \quad (53)$$

The situation for deuterium is more complicated since the equation for $d\mathcal{P}(D)/dt$ cannot be expressed in terms of $\mathcal{P}(D)$. However, the atomic polarization, $\mathcal{A}(D)$, does obey a simple equation. By combining Eqs. (11), (31), (34), and (35), it is possible to show that

$$d\mathcal{A}(D)/dt=\tfrac{1}{2}T_{DB}^{-1}-(T_{DB}^{-1}+T_{D1}^{-1})\mathcal{A}(D) +\tfrac{1}{2}T_{DH}^{-1}[\mathcal{P}(H)-\mathcal{P}(D)]-x_D\,\mathrm{Im}D_{51}e^{-i\omega_0 t}. \quad (54)$$

In order to obtain $\mathcal{P}(D)$ by the stationary solution of Eq. (54), we must relate $\mathcal{P}(D)$ to $\mathcal{A}(D)$. In general, this requires numerical solution of the full set of rate equations. However, in the high-density limit in which the spin-exchange collision rates are much greater than all other relaxation rates, the deuterium populations are given to a good approximation by Eq. (41). In this case, $\mathcal{A}(D)$ and $\mathcal{P}(D)$ are related by Eq. (44). If, in addition, $\mathcal{P}(D)\ll 1$ (a good approximation under the experimental conditions), we can drop the quadratic terms in Eq. (44), and by substituting the result in Eq. (54) we obtain

$$\mathcal{P}(D)=c/d+(2d)^{-1}T_{DH}^{-1}\mathcal{P}(H), \quad (55)$$

where

$$c=\tfrac{1}{2}T_{DB}^{-1}-x_D\,\mathrm{Im}D_{51}e^{-i\omega_0 t}, \qquad d=(11/6)(T_{DB}^{-1}+T_{D1}^{-1})+\tfrac{1}{2}T_{DH}^{-1}. \quad (56)$$

We solve Eqs. (51) and (55) simultaneously for $\mathcal{P}(D)$

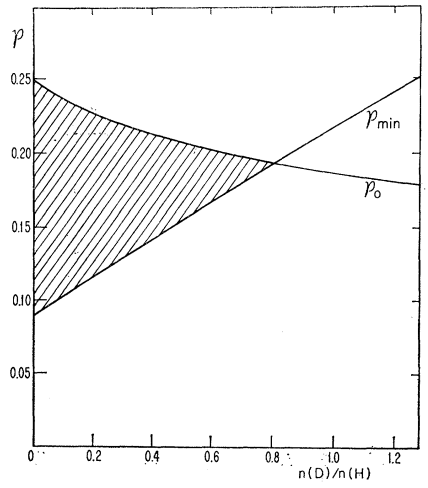

FIG. 3. $\mathcal{P}_0$ and $\mathcal{P}_{\min}$ in terms of the ratio of densities of deuterium and hydrogen. The following typical values are used here: $T_{H1}^{-1}=T_{HB}^{-1}=\sqrt{2}T_{D1}^{-1}=\sqrt{2}T_{D2}^{-1}$, $m=0.2$. Oscillation can occur only if $\mathcal{P}_0>\mathcal{P}_{\min}$, shown by the shaded region.

[19] Note that m is closely related to the parameter q defined by Eq. (11) of Ref. 3. It plays much the same role as a quality factor to describe the experiment.

and $\mathcal{P}(\mathrm{H})$ and substitute the result into Eq. (50). Retaining D_{51} as an independent variable, we obtain in the high-density, low-polarization limit

$$x_H^2=\frac{4}{m}T_{HH}^{-1}\left\{\tau_{H1}^{-1}[\mathcal{P}_0-\mathcal{P}_{\min}]-\frac{n(D)}{n(H)}x_D\,\mathrm{Im}D_{51}e^{-i\omega_D t}\right\}. \quad (57)$$

Here

$$\mathcal{P}_0=\tfrac{1}{2}\tau_{H1}[T_{HB}^{-1}+T_{DB}^{-1}(n(H)/n(D))],$$

$$\mathcal{P}_{\min}=[T_{HH}^{-1}+\tfrac{3}{2}T_{HD}^{-1}]\times[(1+2/m)T_{HH}^{-1}+\tfrac{1}{2}T_{HD}^{-1}]^{-1}, \quad (58)$$

$$\tau_{H1}^{-1}=T_{HB}^{-1}+T_{H1}^{-1}+\frac{11}{6}\frac{n(D)}{n(H)}(T_{DB}^{-1}+T_{D1}^{-1}).$$

$\mathcal{P}_0$ is the equilibrium electron polarization in the absence of rf fields and $\mathcal{P}_{\min}$ is the minimum polarization required for sustained oscillation. In the absence of deuterium, $\mathcal{P}_{\min}=m/(2m+1)\approx 0.1$. $\mathcal{P}_{\min}$ increases with the deuterium density and approaches a limiting value of 3. Since the state selector restricts polarization to 0.5, it is clear that the deuterium density must be limited to avoid completely suppressing oscillation. This limit is illustrated in Fig. 3.

The last term in Eq. (57) is found by substituting the spin exchange equilibrium values of D_{jj} in the equation for D_{51}. The following expression is obtained:

$$x_D\,\mathrm{Im}D_{51}e^{-i\omega_0 t}=\tfrac{1}{6}\mathcal{P}(D)\frac{x_D^2\tau_{D2}^{-1}}{\tau_{D2}^{-2}+(\omega_D-\omega_{0D}')^2}, \quad (59)$$

where

$$\tau_{D2}^{-1}=T_{DB}^{-1}+T_{D2}^{-1}+\tfrac{1}{6}T_{DH}[5-\mathcal{P}(H)]+(11/18)T_{DD}^{-1}[1-\mathcal{P}(D)]. \quad (60)$$

By combining Eqs. (57) and (59) we eventually arrive at

$$x_H^2=\frac{4}{m}T_{HH}^{-1}\tau_{H1}^{-1}\left[\mathcal{P}_0-\mathcal{P}_{\min}\left\{1+\frac{\frac{1}{6}x_D^2}{(\tau_{D1}\tau_{D2})^{-1}+(\tau_{D2}/\tau_{D1})(\omega_D-\omega_{0D}')^2+(\gamma/6)x_D^2}\right\}\right], \quad (61)$$

where

$$\tau_{D1}^{-1}=\frac{n(H)}{n(D)}\tau_{H1}^{-1},$$
$$\gamma=\{1+\tfrac{1}{8}mT_{HH}\tau_{H1}[T_{HH}^{-1}+T_{HD}^{-1}][(1+2/m)T_{HH}^{-1}+\tfrac{1}{2}T_{HD}^{-1}]\}^{-1}, \quad (62)$$
$$\omega_{0D}'=\omega_{0D}-\tfrac{2}{3}[\kappa_{DH}T_{DH}^{-1}+\tfrac{2}{3}\kappa_{DD}T_{DD}^{-1}].$$

The fractional change in radiated power due to the application of the field x_D is then

$$\frac{\delta P}{P}=\frac{\mathcal{P}_{\min}}{\mathcal{P}_0-\mathcal{P}_{\min}}\times\frac{\frac{1}{6}x_D^2}{(\tau_{D1}\tau_{D2})^{-1}+(\tau_{D1}/\tau_{D2})(\omega_D-\omega_{0D}')^2+(\gamma/6)x_D^2}. \quad (63)$$

Equation (63) describes a Lorentzian resonance line. Since $\gamma<1$, the effect of power broadening is suppressed compared to the usual case. This occurs because spin-exchange links angular momentum in the cavity radiation field with the atomic spin systems. The applied deuterium signal broadens the line as it decreases the population difference. However, at the same time the flow of angular momentum to the hydrogen radiation field decreases, and the net effect is that the radiation field behaves like an angular momentum reservoir which partially restores the difference.

The amplitude of the line is enhanced by the factor $\mathcal{P}_{\min}/(\mathcal{P}_0-\mathcal{P}_{\min})$. This reflects the fact that when the oscillation is marginal, arbitrarily small influences can produce significant changes in the oscillation level. In one sense, this effect tends to amplify the resonance. However, since it also makes the system unstable in the presence of small fluctuations of flux or linewidth, it is the source of a number of experimental difficulties.

The resonance maximum is shifted from the true resonance frequency by an amount

$$\delta\omega=\omega_{0D}'-\omega_{0D}=-\tfrac{2}{3}[\kappa_{DH}T_{DH}^{-1}+\tfrac{2}{3}\kappa_{DD}T_{DD}^{-1}]. \quad (64)$$

Bender has calculated κ_{HH} in the classical limit[10] and finds $\kappa_{HH}=-0.25$. A preliminary experimental determination[14] yields $\kappa_{HH}=-0.4\pm0.3$. If we make the reasonable assumption that

$$\kappa_{HH}=\kappa_{HD}=\kappa_{DH}=\kappa_{DD}=-0.4,$$
$$T_{HH}^{-1}=T_{HD}^{-1}=T_{DH}^{-1}=T_{DD}^{-1}=\tfrac{1}{2}\tau_{H2}^{-1},$$
$$m=0.2 \quad \text{and} \quad \mathcal{P}=0.25,$$

we find that $\delta\omega$ is approximately 1% of the linewidth of the hydrogen resonance, $(\pi\tau_{H2})^{-1}$.

Some comments on the approximations made in deriving Eq. (63) are in order. This result assumes that the system is in spin exchange equilibrium, i.e., spin-exchange rates are large compared to the rates of all other mechanisms which influence the populations. The only effect of these mechanisms, including radiation, is to determine the spin temperature of the system. When

we make the further assumption that the polarization is small, the problem effectively reduces to that of a two-level system. In practice, spin-exchange equilibrium was not reached with the available beam flux (nor is it necessarily true that this limit was desirable, since signal strength would have been increased at the expense of increased linewidth). Nevertheless, at collision rates high enough to provide effective coupling of the two spin systems, the result is useful in providing a simple description of the physical processes occurring and in making estimates of such effects as spin-exchange frequency shifts.

The results of a similar analysis for the field-independent transitions are given in Appendix A. It is also possible to detect the deuterium resonance when the maser is below the hydrogen oscillation threshold by using the maser as an amplifier. This method is described in Appendix B.

IV. APPARATUS

Since the hydrogen maser has been described elsewhere,[3] only features new to this experiment are described here.

Magnetic Field

The static field H_0 is perpendicular to the cavity axis and is produced by a cylindrical current sheath shaped so as to produce a current density with an azimuthal dependence approximating $\sin\theta$. The sheath is surrounded by three cylindrical shields (similar to those described in Ref. 3), and satisfactory oscillation is obtained at fields as low as 0.1×10^{-3} G. Under favorable ambient conditions, fluctuations of the field during successive 10-sec periods are 2×10^{-8} G, corresponding to mean frequency fluctuations of the maser of 0.03 cps.

Source

It can be seen from Eq. (63) that the hydrogen oscillation level depends critically on $\mathcal{P}_{\min}$. Since $\mathcal{P}_{\min}$ depends on the H-D spin exchange rate, the oscillation level is very sensitive to fluctuations in the source pressure. Because the usual pressure reducers at the gas storage tanks allow fluctuations in the flow rate of up to 10%, the handling system shown in Fig. 4 was finally adopted. The source gases are stored in reservoir tanks at twice atmospheric pressure, and the flow rate is adjusted by variable leaks. The flow rate is smoothed by a filter composed of a reservoir and small fixed leak. The time constant of the system is approximately 5 min.

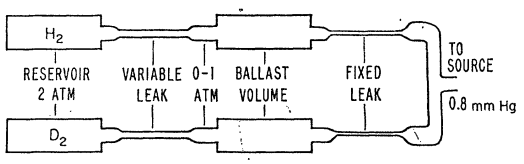

FIG. 4. Gas-handling system.

Rf Driving Field

The 327-Mc/sec rf field for driving deuterium resonances is obtained by X15 frequency multiplication of a 21.8-Mc/sec signal from a Rohde and Schwarz type XUA frequency synthesizer. Coupling is achieved by a half-wavelength lumped transmission line as shown in Fig. 5. In order to keep the rf amplitude constant as the frequency is swept, the field is sampled by a small loop and the resultant signal is rectified and applied to a gain control on the driver. The frequency of the 327 Mc/sec driving field is monitored by a HP 5243L frequency counter with a time base provided by a General Radio 1120-AH frequency standard maintained by J. A. Pierce.

Processing of the Maser Signal

The system illustrated in Fig. 6 provides a record of both the amplitude and frequency of the maser signal. (The frequency is needed to determine the ambient magnetic field.) Power is coupled from the cavity, converted to approximately 30 Mc/sec and amplified. A second stage of conversion reduces the frequency to approximately 6 kc/sec, where it is detected and displayed by a recorder. The oscillation frequency is determined by using a second hydrogen maser as a frequency reference. Both systems use the same local oscillator to convert the signals to 30 Mc/sec where they are mixed. The difference frequency (approximately 250 cps) is measured by a counter.

V. Procedure and Results

The procedure for detecting a deuterium resonance was to adjust the hydrogen density to several times its threshold value and then to increase the deuterium density until the radiated power level was reduced by about 25%. The degree of spin exchange equilibrium was investigated by sweeping the entire deuterium spectrum for $\Delta m_F=-1$ hyperfine transitions. The ratio of the intensity of the transition $(\frac{3}{2},\frac{3}{2})\rightarrow(\frac{1}{2},\frac{1}{2})$ to the field-independent transitions was found to be 3.3. It can be shown that in the high-density limit the ratio should be approximately $\frac{3}{2}(1+\mathcal{P})/(1-\mathcal{P})$, and that in the low-density limit it should be ∞. For the reasonable value $\mathcal{P}=\frac{1}{4}$, the predicted high-density ratio is 2.5, which indicates that the system was in an intermediate

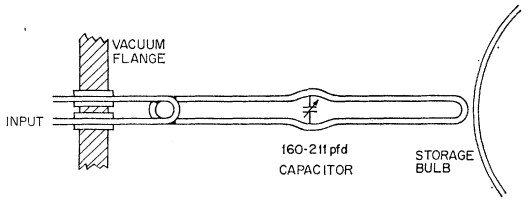

FIG. 5. Schematic diagram of the lumped transmission line used to couple the deuterium driving field.

situation approaching spin exchange equilibrium. Failure to observe the transition $(\frac{1}{2}, -\frac{1}{2}) \rightarrow (\frac{3}{2}, -\frac{3}{2})$ is consistent with this conclusion.

Observations of the Field-Dependent Transition $(\frac{3}{2},\frac{3}{2}) \rightarrow (\frac{1}{2},\frac{1}{2})$

Figure 7 shows a trace of resonance on this transition made under favorable conditions of magnetic field and beam stability. The maximum ratio $\delta P/P$ is 0.4, and the amplitude signal-to-noise ratio is estimated to be 10:1. The Lorentz curve fitted to the data has a width of 7.0 cps, of which it is estimated that 5.0 cps is due to spin exchange. The duration of the line sweep was about 2 min. The estimated uncertainty in locating the center of the curve is 0.2 cps. The magnetic field was determined from the frequency of the hydrogen oscillation, which was monitored continuously during the run, and the results were corrected to zero magnetic field by using the Breit-Rabi formula. This correction was typically 250 cps.

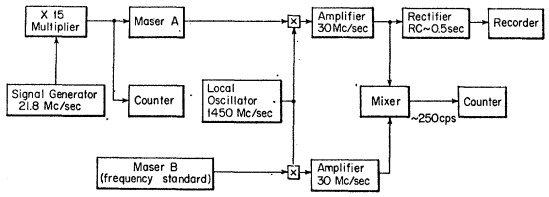

FIG. 6. Block diagram of the detection system. Maser A is the experimental apparatus. Its amplitude is monitored to display the deuterium resonance, and its frequency is simultaneously monitored against maser B to measure the magnetic field.

A histogram showing the results of 30 determinations is shown in Fig. 8. Each determination consisted of two sweeps of the line in opposite directions. The standard deviation of the mean is 0.1 cps. In addition, uncertainties are contributed by possible spin exchange frequency shifts and by cavity mistuning. The former were estimated in Sec. III to be about 1% of the linewidth, or 0.1 cps. The effect of cavity mistuning is more serious. The hydrogen oscillation frequency is pulled by an amount equal to the cavity tuning error divided by the ratio of cavity linewidth to atomic resonance line width. The cavity was tuned by conventional means to about 500 cps, but could drift by as much as 1 kc/sec during a run. Assuming a cavity resonance width of 30 kc/sec, and an atomic resonance width of 10 cps, the limit of error in the oscillation frequency is 0.33 cps. Since the magnetic field correction for deuterium is $\frac{4}{3}$ that of hydrogen, this places a limit of error on the deuterium frequency of 0.45 cps.

The total uncertainty in this determination due to all the above sources is taken to be 0.5 cps.

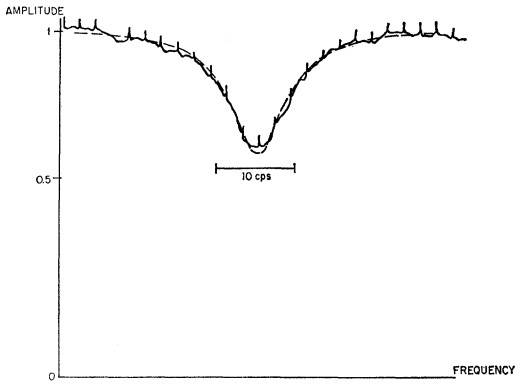

FIG. 7. Trace of the recorder output of a scan of the deuterium transition $(\frac{3}{2},\frac{3}{2}) \rightarrow (\frac{1}{2},\frac{1}{2})$. The dashed line is the plot of an amplitude curve corresponding to a Lorentz power curve. The vertical breaks are frequency markers.

Observations of the Field-Independent Transitions $(\frac{3}{2},\frac{1}{2}) \rightarrow (\frac{1}{2}, -\frac{1}{2})$ and $(\frac{1}{2},\frac{1}{2}) \rightarrow (\frac{3}{2}, -\frac{3}{2})$

Because of the low signal-to-noise ratio available with these transitions, measurements were made by manually adjusting the frequency to the center of the resonance line rather than by sweeping the whole curve. The results of 25 observations taken over a 10-min interval are shown in Fig. 8. The total splitting of the two unresolved transitions due to magnetic field is 0.2 cps. If the components have the same intensity, no error is introduced. Since the system is not in spin-exchange equilibrium, one component may predominate, but since the maximum error due to this case is 0.1 cps, it will be neglected. Similarly, the spin-exchange shifts should cancel and are neglected. The total uncertainty in this determination is taken to be the statistical error, 0.3 cps.

Collisions of the deuterium with the storage-bulb wall introduce a frequency shift in all of the transitions observed, but this can be neglected on the following grounds: For a storage bottle with the same dimensions and wall coating material, the shift in the hydrogen $\Delta m=0$ hyperfine resonance has been measured to be -0.0298 cps.[20] Determinations of pressure shifts of the

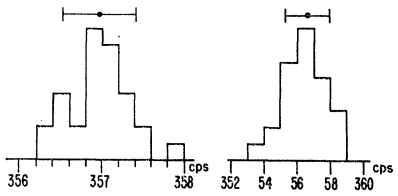

FIG. 8. Histogram of the results. The left-hand plot is for the field-dependent transition $(\frac{3}{2},\frac{3}{2}) \rightarrow (\frac{1}{2},\frac{1}{2})$, while the right-hand plot is for the field-independent transitions $(\frac{3}{2},\frac{1}{2}) \rightarrow (\frac{1}{2}, -\frac{1}{2})$, and $(\frac{1}{2}, -\frac{1}{2}) \rightarrow (\frac{3}{2}, -\frac{3}{2})$. The abscissa labels are in cycles per second and represent the last digits of 327 384 000 cps. The mean value, and rms deviation are indicated.

[20] S. B. Crampton, D. Kleppner, and N. F. Ramsey, Phys. Rev. Letters 11, 338 (1963).

hydrogen isotopes in optical-pumping experiments lead to approximately equal fractional shifts for a variety of buffer gases. Assuming that this result also holds true for wall collisions, the wall shift for deuterium is -0.007 cps, which is negligible compared to the final uncertainty.

To transfer the measurements of Fig. 8 from the $UT2$ to the $A1$ time scale, the results must be decreased by 4.25 cps. By combining the two determinations with a weighting proportional to the inverse squares of their uncertainties, we obtain the final result

$$\Delta\nu(D)=327\ 384\ 352.3\pm0.25\ \text{cps},$$

assuming that

$$\Delta\nu(\text{Cs})=9\ 192\ 631\ 770\ \text{cps}.$$

This result is higher than the previous optical pumping result of Anderson, Pipkin, and Baird[8] by their experimental error, 5 cps.

APPENDIX A: DETECTION OF FIELD-INDEPENDENT DEUTERIUM RESONANCES

In addition to the field-dependent transition already described, $(\frac{3}{2},\frac{3}{2})\rightarrow(\frac{1}{2},\frac{1}{2})$, the field-independent transitions $(\frac{3}{2},\frac{1}{2})\rightarrow(\frac{1}{2},-\frac{1}{2})$ and $(\frac{1}{2},\frac{1}{2})\rightarrow(\frac{3}{2},-\frac{1}{2})$ are also of interest. Actually, these transitions possess a first-order field dependence due to the nuclear interaction with the external field, but at the fields used, this is much less than the linewidth. At spin-exchange equilibrium, the intensities of the two lines are equal, and the resulting line lies at the zero field average.

The procedure for analyzing these transitions is similar to that used above. In the same limits of high density and low polarization, the transitions undergo spin-exchange frequency shifts given by

$$\begin{aligned}\delta\omega[(\tfrac{3}{2},\tfrac{1}{2})\rightarrow(\tfrac{1}{2},-\tfrac{1}{2})]&=\frac{2}{27}\mathcal{P}\kappa_{DD}T_{HD}^{-1},\\ \delta\omega[(\tfrac{1}{2},\tfrac{1}{2})\rightarrow(\tfrac{3}{2},-\tfrac{3}{2})]&=-\frac{2}{27}\mathcal{P}\kappa_{DD}T_{HD}^{-1}.\end{aligned}\tag{A1}$$

The shifts average to zero. The result for the detected signal is

$$\frac{\delta P}{P}=\frac{\mathcal{P}_{\min}}{\mathcal{P}_{\min}-\mathcal{P}_0}\times\frac{x_D^2/9}{(\tau_{D1}\tau_{D2})^{-1}+(\tau_{D2}/\tau_{D1})(\omega_D-\omega_{D0})^2+(\gamma/9)x_D^2},\tag{A2}$$

where x_D is given by Eq. (10).

APPENDIX B: MASER DETECTION BELOW THE OSCILLATION THRESHOLD

If $\mathcal{P}_0<\mathcal{P}_{\min}$, self-sustained oscillation will not occur. However, it is still possible to detect deuterium resonances by using the maser as an amplifier. A small rf field is applied to the hydrogen at its resonance frequency, and the intensity of the stimulated radiation is monitored. If the power level of the applied rf field is below saturation and the frequency is well within the hydrogen bandwidth, the high-density low-polarization solution resembles the oscillator solution. We will let $\mathcal{P}$ denote the power detected when the hydrogen is radiating minus the power detected when there is no hydrogen present. For the case of hydrogen radiating on the transition $(1,1)\rightarrow(0,0)$, the change in P due to driving the deuterium transition $(\frac{3}{2},\frac{3}{2})\rightarrow(\frac{1}{2},\frac{1}{2})$ is

$$\frac{\delta P}{P}=\left(\frac{\mathcal{P}_{\min}}{\mathcal{P}_{\min}-\mathcal{P}_0}\right)\frac{x_D^2/6}{(\tau_{D1}\tau_{D2})^{-1}+(\tau_{D2}/\tau_{D1})(\omega_D-\omega_{0D}')^2+(\mathcal{P}_{\min}/\mathcal{P}_{\min}-\mathcal{P}_0)(x_D^2/6)},\tag{B1}$$

where the symbols have the definitions given in Sec. III. Due to the factor $\mathcal{P}_{\min}/(\mathcal{P}_{\min}-\mathcal{P}_0)$ in the power-broadening term, the fractional signal change on resonance is less for the amplifier than for the oscillator. There are two reasons for this; the system is no longer marginally oscillating, and the hydrogen field no longer acts as a polarization reservoir. Furthermore, with this method the hydrogen frequency cannot be used to monitor the magnetic field. There is, however, a compensating advantage which may make detection below threshold useful in some circumstances. When the oscillation condition $\mathcal{P}_0>\mathcal{P}_{\min}$ is relaxed, T_{HB}^{-1} and T_{DB}^{-1} may be reduced to allow detection at lower overall linewidths. If the signal-to-noise ratio is limited primarily by beam and magnetic field stability, magnetic-field-independent transitions may be detected with increased sensitivity using the maser as an amplifier.